Annals of Nuclear Energy 108 (2017) 42–56

Contents lists available at ScienceDirect

Annals of Nuclear Energy

journal homepage: www.elsevier.com/locate/anucene

Structural analysis of the CAREM-25 nuclear power plant subjected to the design basis accident and seismic loads

Daniel Ambrosini *, Ramón H. Codina, Oscar Curadelli, Carlos A. Martínez

Engineering Faculty, National University of Cuyo, CONICET, Mendoza, Argentina

ARTICLE INFO

Article history:
Received 18 October 2016
Accepted 20 April 2017

Keywords:
CAREM-25 nuclear power plant
Transient thermo-mechanical analysis
Seismic analysis
Finite element model
Design basis accident

ABSTRACT

In this paper, a numerical study about the structural response of the Argentine nuclear power plant CAREM-25 subjected to the design basis accident (DBA) and seismic loads is presented. Taking into account the hardware capabilities available, a full 3D finite element model was adopted. A significant part of the building was modeled using more than 2 M solid elements. In order to take into account the foundation flexibility, linear springs were used. The springs and the model were calibrated against a greater model used to study the soil-structure interaction. The structure was subjected to the DBA and seismic loads as combinations defined by ASME international code. First, a transient thermal analysis was performed with the conditions defined by DBA and evaluating the time history of the temperature of the model, each 1 h until 36 h. The final results of this stage were considered as initial conditions of a static structural analysis including the pressure defined by DBA. Finally, an equivalent static analysis was performed to analyze the seismic response considering the design basis spectra for the site. The different loads were combined and the abnormal/extreme environmental combination was the most unfavorable for the structure, defining the design.

1. Introduction

Thermo-mechanical and seismic effects evaluation of building and containment structures in nuclear power plants (NPP) is essential for structural design of this kind of structures (Yu et al., 2015; Kwak and Kwon, 2016). Based on simulation and numerical results, it is possible to analyze the stress state of concrete structures under thermal, mechanical and seismic loads in NPP in order to design the reinforcement as well as to prevent failures.

CAREM-25 is a modern prototype of nuclear power plant, which it is located at the north of the province of Buenos Aires (Argentina). The reactor was integrally designed by CNEA (National Atomic Energy Commission) and is basically a simplified pressurized water reactor (PWR) designed to have an electrical output of 25 MW for the first prototype. The whole high-energy primary system, core, steam generators, primary coolant and steam dome, is contained inside a single pressure vessel. Moreover, this nuclear plant has an indirect cycle reactor with some distinctive and characteristic features which greatly simplify the design, and also contributes to a higher safety level. Some of the high-level design characteristics of the plant are: an integrated primary cooling system, natural circulation and self-pressurization of the primary system. The pressure value in CAREM-25 is achieved by balancing the vapor production in the core plus chimney sections and the condensation of vapor in contact with cold structures in the upper steam dome (Marcel et al., 2013; Delmastro, 2000; Boado Magan et al., 2011).

The main objectives of this paper are to present the structural response of the concrete reactor containment of CAREM-25 subjected to thermal, mechanical and seismic loading, and to provide modeling guidelines for numerical structural analysis of concrete NPPs. For this purpose, a full 3D numerical model was developed and transient thermal and static structural analyses were performed.

2. Numerical model

The numerical model was performed following the structural and architectural plans of the actual building of the CAREM-25 NPP, according to the CNEA documentation. A commercial general purpose code was used with this objective (ANSYS 2010). Large attention was focused on selection of geometry, mesh density and definition of boundary conditions.

* Corresponding author at: Facultad de Ingeniería. Centro Universitario, Parque Gral. San Martín, 5500 Mendoza, Argentina.
E-mail address: dambrosini@uncu.edu.ar (D. Ambrosini).

http://dx.doi.org/10.1016/j.anucene.2017.04.029
0306-4549/

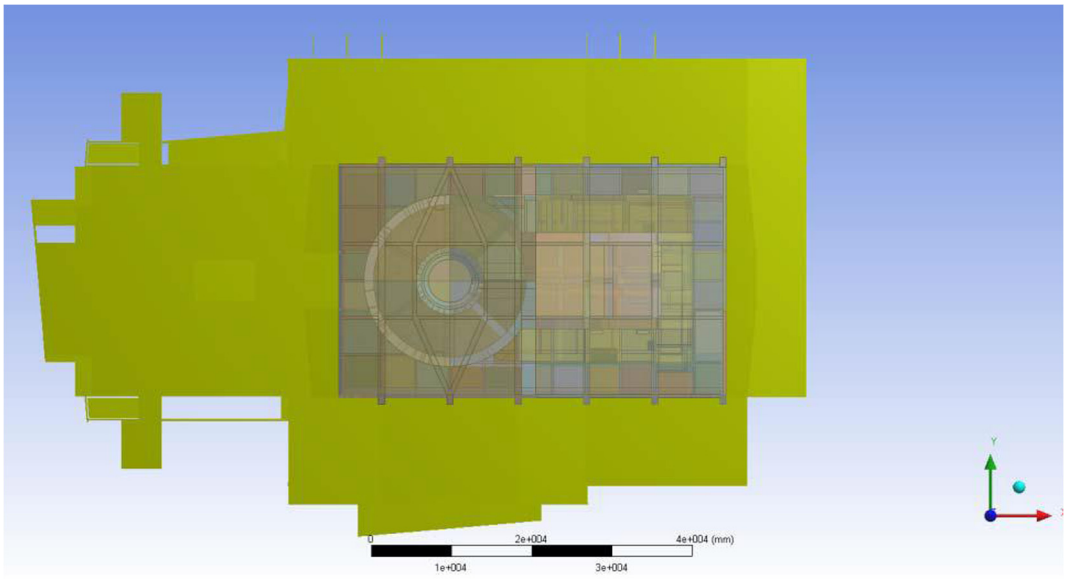

Fig. 1. Plan view of the whole building and the part that is considered in the model.

Fig. 2. Geometry of the simplified model.

Table 1
Maximum Principal Stress for different element sizes. Cylinder without holes.

Element size	Maximum Principal Stress (Pa)
50 cm	2.6093e7
25 cm	2.6093e7
12.5 cm	2.6102e7
6.25 cm	2.6110e7

Fig. 3. Finite element model mesh.

2.1. Geometry selection

A previous analysis of the entire building was carried out in order to define the part that provide significant stiffness to the structure and influence the structural response. The part of the whole building that is considered in the model is presented in Fig 1.

Considering the results of modal analysis, presented in section 4.2, it could be verified that the selection of the building considered in the model was acceptable.

2.2. Element types

After analyzed the alternatives of different types of elements available in ANSYS Mechanical (2010) it was decided to use the following elements: For thermal analysis, solid elements with 20 and 10 nodes with a single degree of freedom, temperature, at each node (SOLID90 and SOLID87 ANSYS, 2010). For structural analysis, SOLID186 and SOLID187 (ANSYS, 2010) were used. These elements are defined by 20 and 10 nodes respectively, having three degrees of freedom at each node: translation in the nodal x, y, and z directions.

Material properties of the concrete were defined as: Density: $\rho = 2400\ kg/m^3$, Young's modulus: $E = 30{,}000$ MPa, Poisson's ratio: $\mu = 0.18$. Regarding a key parameter as the coefficient of thermal

Fig. 4. Longitudinal section of the FEM model by XZ plane.

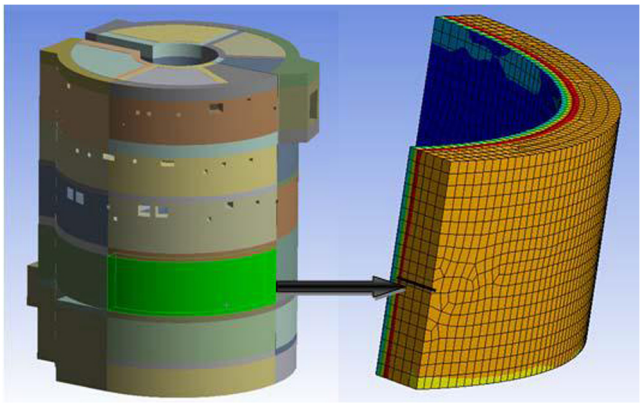

Fig. 5. Zone of the containment free of holes and geometric discontinuities.

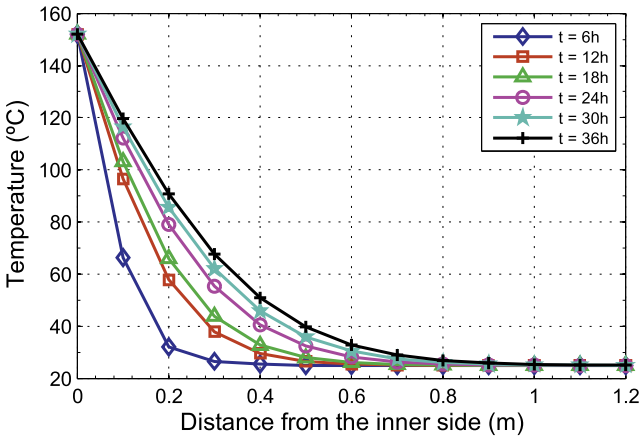

Fig. 6. Temperature in the wall thickness of the containment.

Table 2
Soil stiffness coefficients (MN/m^3).

	Deepest foundation level −12.50 m level	Shallow foundation level −5.80 m level
Vertical stiffness coefficient K_V	30.64	11.35
Horizontal stiffness coefficient K_X	17.70	21.10
Horizontal stiffness coefficient K_Y	64.20	45.10

expansion, it was adopted as $\alpha = 1\ 10^{-5}\ 1/°C$, according to recommendations and studies from ACI (2007), ACI (2001), Neville (1995), Willam et al. (2009), Li et al. (2002) and Uygunoglu and Topçu (2009).

2.3. Mesh density

Before conducting structural and thermal analysis, a series of preliminary studies were performed in order to determine the influence on the solution of mesh sizes. Four simplified models with different element sizes were performed (Fig. 2): 50 cm; 25 cm; 12.5 cm and 6.25 cm. The cylinder has dimensions in plan similar to the containment of the actual structure: 21.4 m of external diameter, 10 m height and thickness of the wall of 1.2 m.

Table 3
Evolution of pressure and temperature for different DBAs.

		Dry Containment	Suppression Pool	Pool HRSS 1	Pool HRSS 1
1-Envelope condition (EC)	Pressure (MPa)	0.50	0.50	0.50	0.50
	Temp (°C)	152.0	152.0	152.0	152.0
2-LOCA of the dry containment (LOCA)	Pressure (MPa)	0.50	0.46	0.31	0.31
	Temp (°C)	152.0	149.3	136.3	136.3
3- Spurious opening of the safety valve (SOSV)	Pressure (MPa)	0.10/36 * t + 0.10	0.10/36 * t + 0.15	0.10	0.10
	Temp (°C)	0.5611 * t + 100.6	0.4444 * t + 111.8	100.0	100.0
4-Rupture of the tube of the condenser of the HRSS (RTC)	Pressure (MPa)	0.50	0.46	0.50	0.31
	Temp (°C)	152.0	149.3	152.0	136.3
5-Loss of the cold source (LCS)	Pressure (MPa)	0.15/36 * t + 0.10	0.15/36*t + 0.15	0.15/36 * t + 0.19	0.10 if t ≤ 24 h 0.15/36 * (t − 24) + 0.1 if t > 24 h
	Temp (°C)	0.7611 * t + 101.2	0.6167*t + 112.1	0.5361 * t + 119.2	100.0 if t ≤ 24 h 0.95 * (t − 24) + 100 if t > 24 h

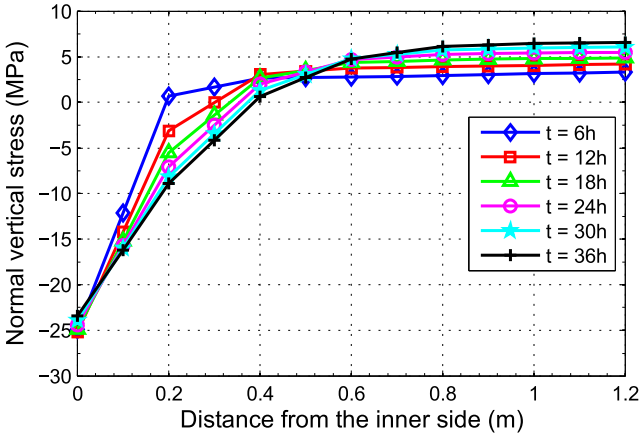

Fig. 7. Normal vertical stresses in the wall thickness of the containment.

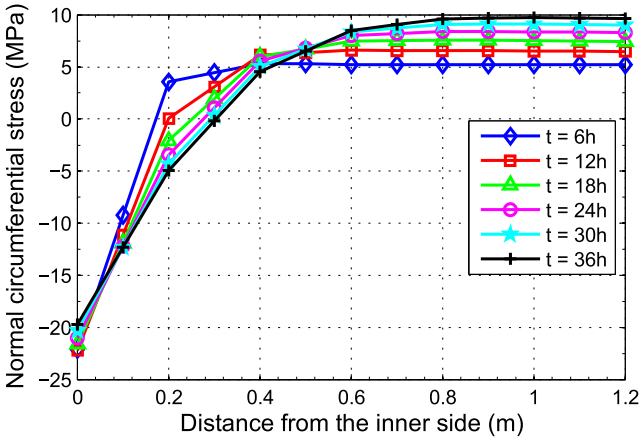

Fig. 8. Normal circumferential stresses in the wall thickness of the containment.

Table 4
Modal analysis results. Natural Frequencies (Hz).

Mode	Complete model Ambrosini et al., 2014	Reduced Model This paper	Difference
Translational X	1,79	2,02	12,8%
Translational Y	2,04	2,22	8,8%

It was considered only thermal load because this state is that which produces the greatest stresses. A linear transient thermal analysis was performed with constant internal temperature of 155 °C and initial and outer temperature of 25 °C. The duration of the analysis was 36 h since it was more unfavorable. With the results of the thermal analysis, a linear static structural analysis was performed. In this case, base fixed support was considered as boundary condition.

Table 1 shows maximum principal stress for each mesh density.

As can be seen, virtually no differences were found in the maximum principal stresses. According to this result, it can be concluded that the mesh adopted, with elements of 20 cm, it is suitable for the stress study. Thus, the model has 2,008,793 elements and 8,864,261 nodes (Figs. 3 and 4).

2.4. Boundary conditions

In order to represent the flexibility of the soil, elastic support boundary conditions on the surfaces of slabs and walls in contact with the ground were admitted in the reduced model. These conditions are based on a foundation stiffness, which is defined as the pressure required producing a unit normal deflection of the foundation.

As a first approximation, the coefficients of soil stiffness were obtained through a model of rectangular foundation defined by Wolf and Somaini (1986). Here, these coefficients are functions of soil properties (shear modulus, density and Poisson's ratio), size of the foundation and the depth at which the foundation is located. Because of this, different coefficients were defined for the deepest

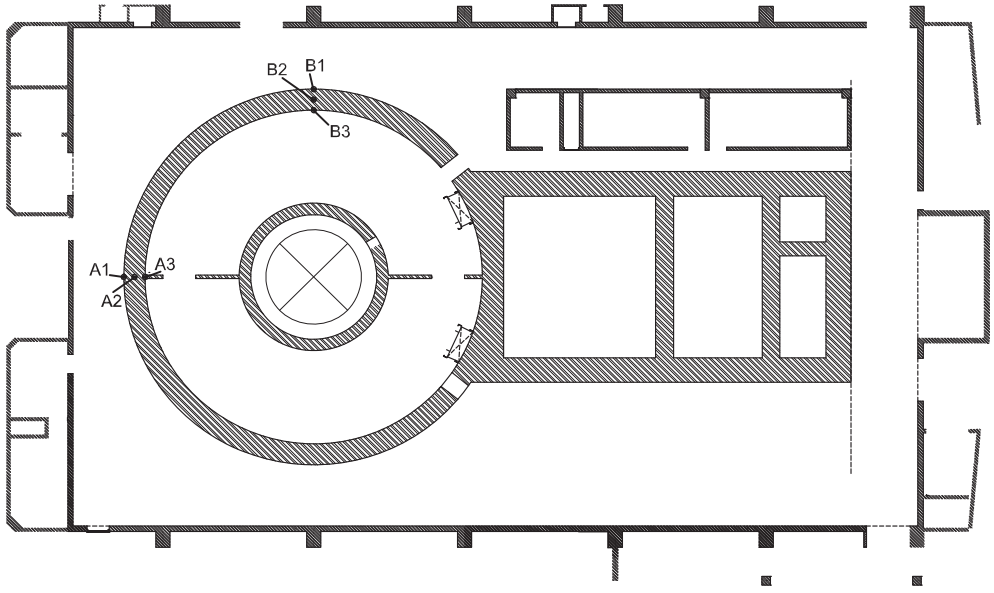

Fig. 9. Plan view of the considered axes.

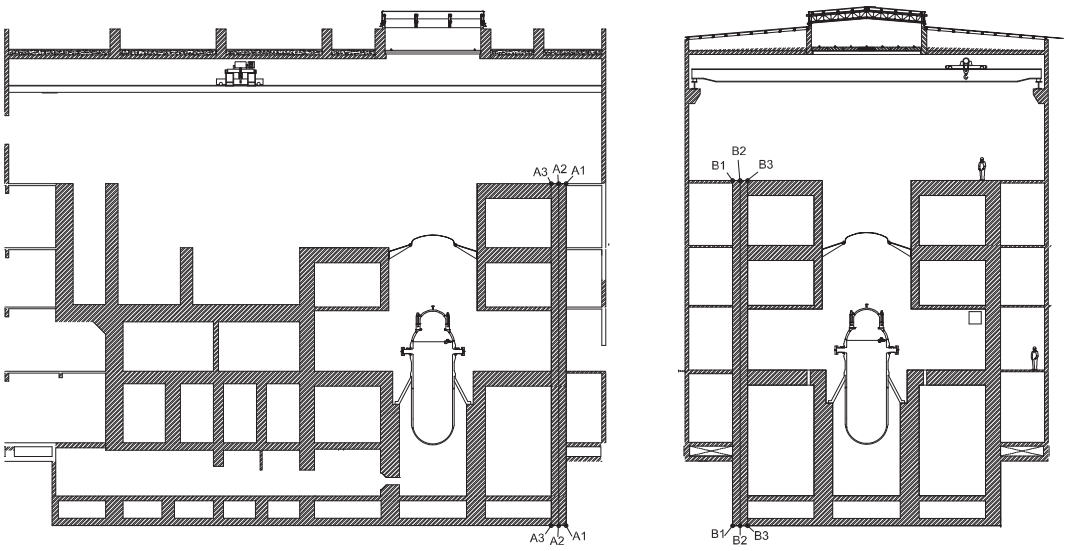

Fig. 10. Section views of the considered axes.

(a) Normal vertical stresses. Outer face

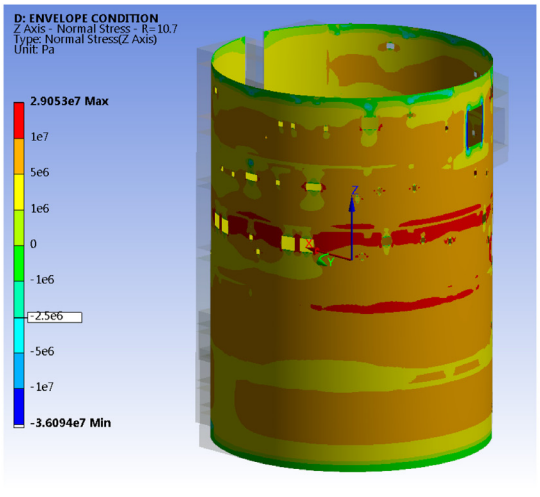

(b) Normal circumf. stresses. Outer face

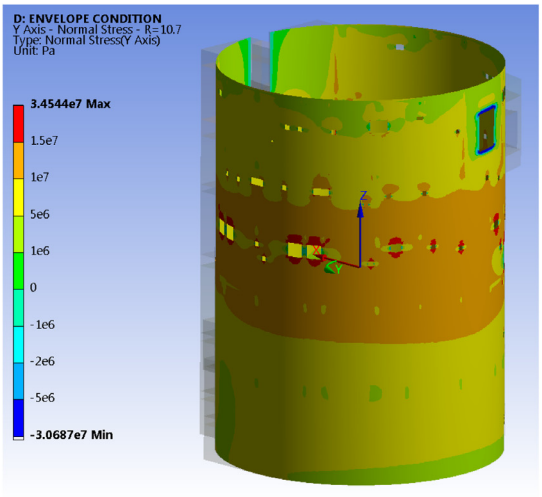

(c) Normal vertical stresses. Inner face

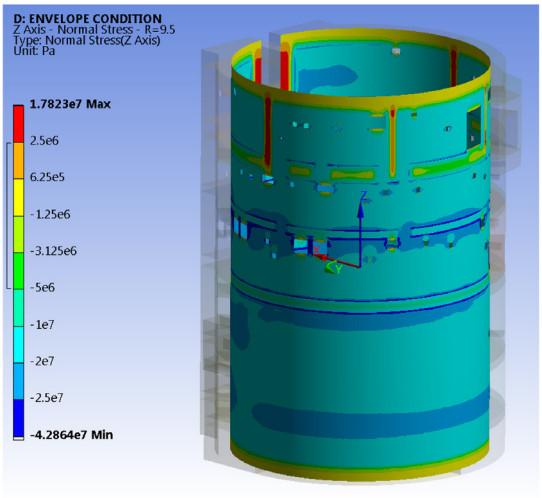

(d) Normal circumf. stresses. Inner face

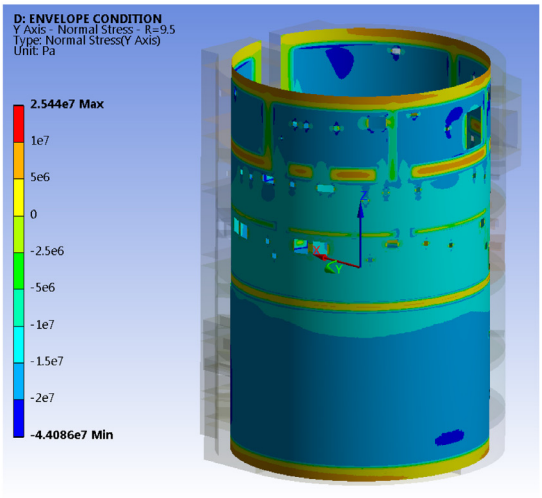

Fig. 11. Vertical and circumferential stresses. Inner and outer faces of the containment wall.

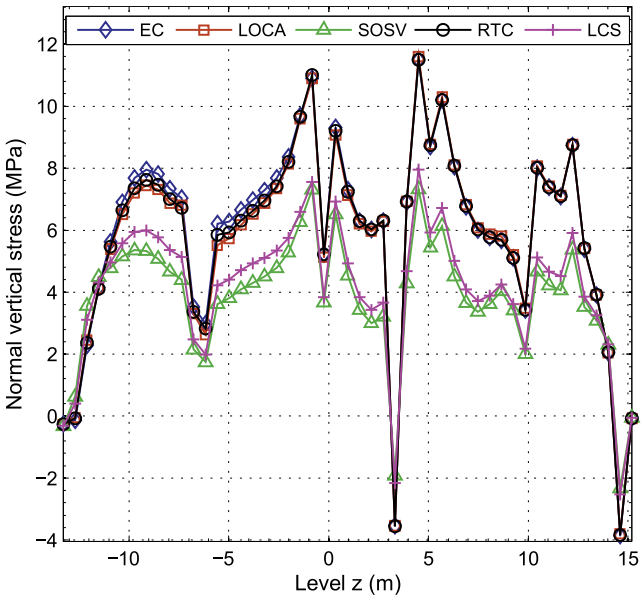

Fig. 12. Normal vertical stress. A1.

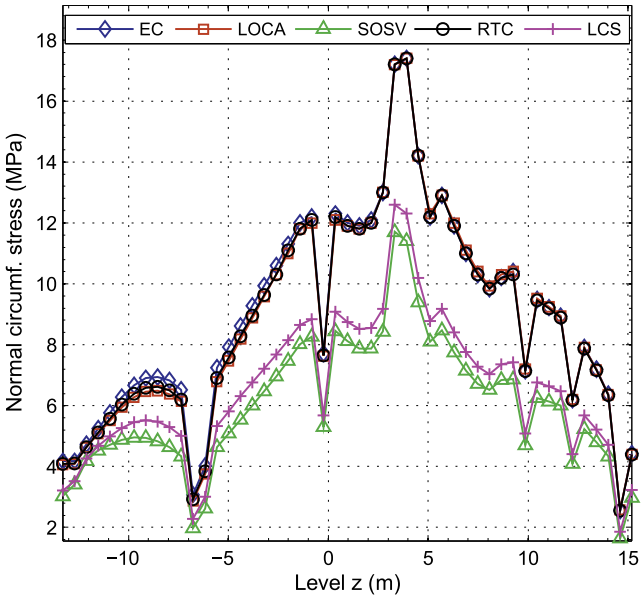

Fig. 13. Normal circumferential stress. A1.

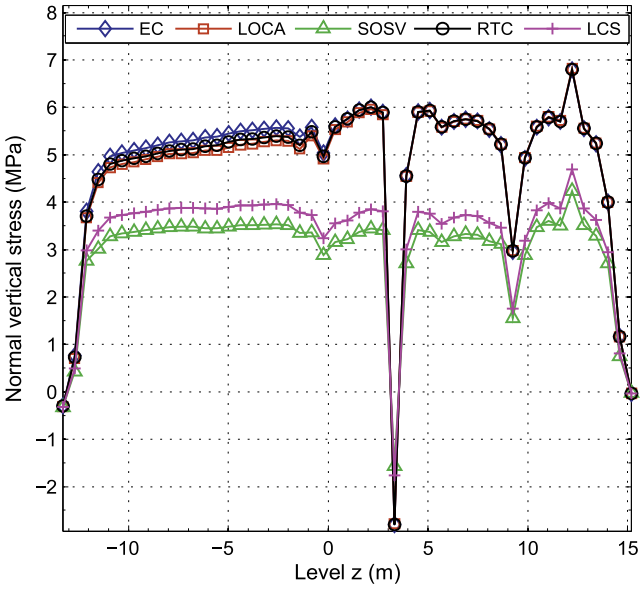

Fig. 14. Normal vertical stress. A2.

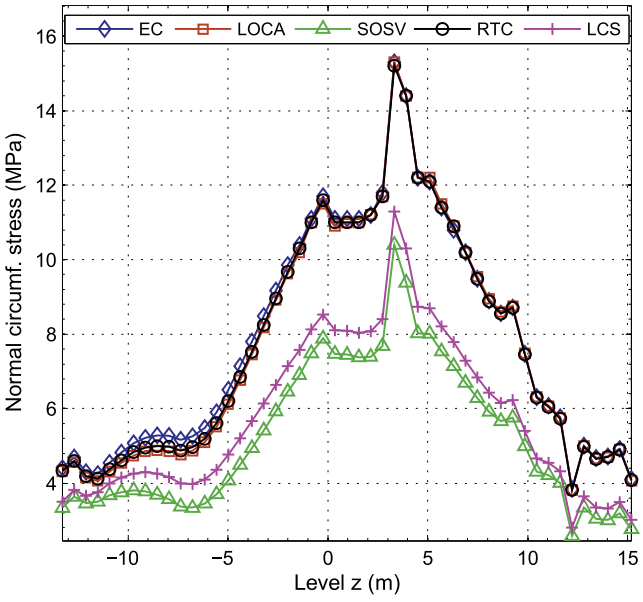

Fig. 15. Normal circumferential stress. A2.

foundation level (-12.50 m) and the shallow foundation level (-5.80 m). At a later stage, these coefficients were adjusted to obtain natural frequencies of the reduced model close to those obtained for the full model used in a previous analysis of Soil-Structure Interaction (SSI) (Ambrosini et al., 2014). In Table 2 the final calibrated coefficients are presented.

3. Load cases definition

3.1. Design basis accident loads

The following Design Base Accidents (DBAs) were considered, according to CNEA reports (CNEA 2011, 2012a, 2012b, 2013):

1) Envelope condition (EC)
2) Loss of coolant accident (LOCA) of the primary system of the Dry Containment (DC)
3) Spurious opening of the safety valve of the Reactor Pressure Vessel (RPV): loss of coolant in the primary system with direct discharge into the Suppression Pool (SP)
4) Loss of coolant of the primary system by rupture of one tube of the condenser of the Heat Removal Security System (HRSS) into the pool of the same system.
5) Loss of Cold Source, by loss of the main power of the steam generators, with action of the HRSS as unique removal system of heat of the RPV.

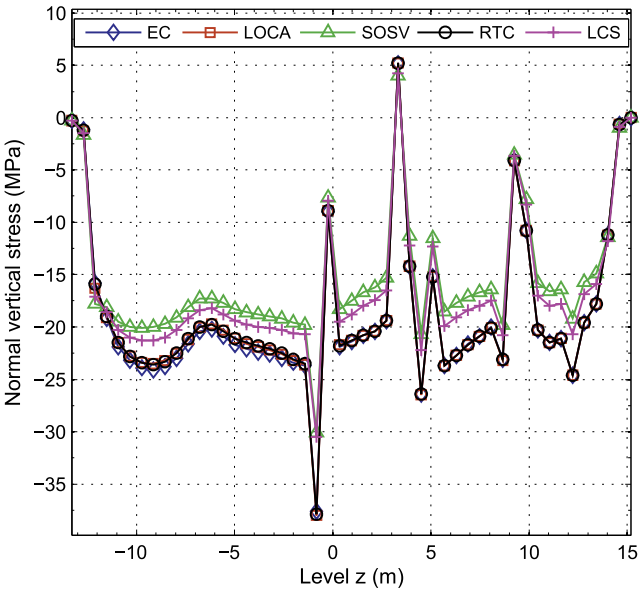

Fig. 16. Normal vertical stress. A3.

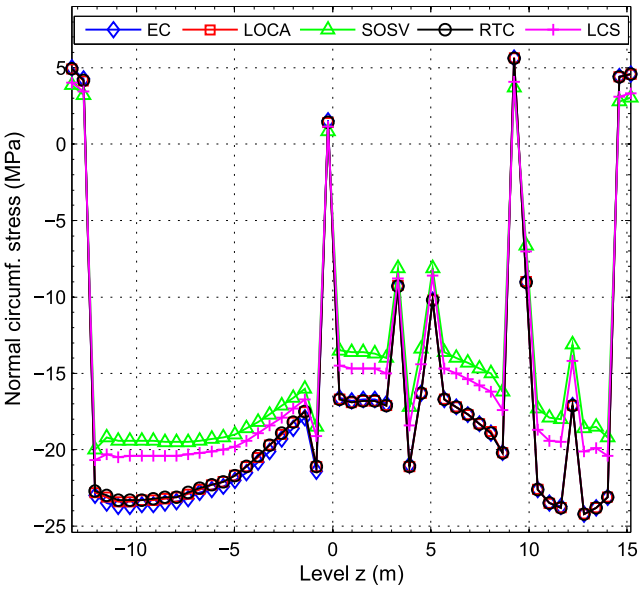

Fig. 17. Normal circumferential stress. A3.

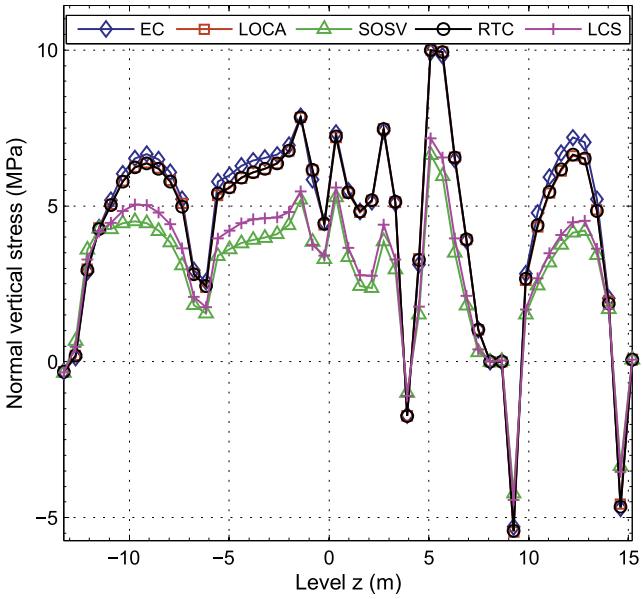

Fig. 18. Normal vertical stress. B1.

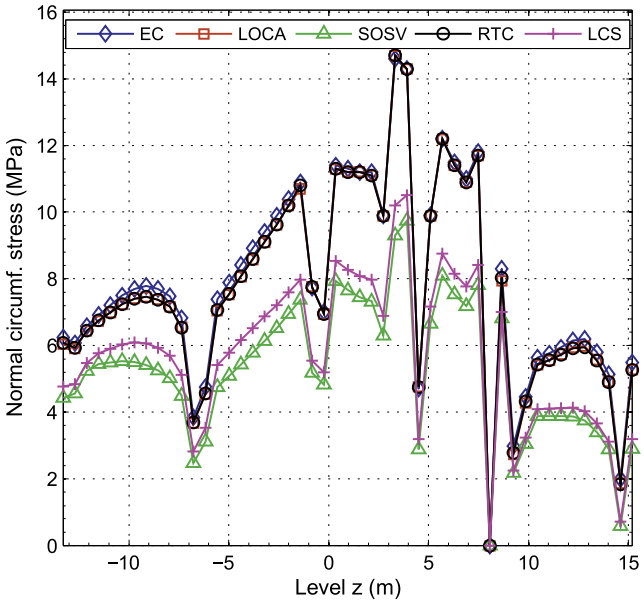

Fig. 19. Normal circumferential stress. B1.

The envelope condition respect to the values of pressure and temperature obtained consist in considering a constant design pressure (5 bar) and a saturation temperature corresponding to this pressure (152 °C) during 36 h in all the containment, reaching such values instantaneously (CNEA, 2012a). This case could be considered as a strongly conservative case.

Since in all events the first pressurization occurs in a relatively short time, that is negligible from the viewpoint of the thermal inertia of concrete, it is considered in all cases an instantaneous pressurization in the initial instant t = 0 to the value in that a marked decrease is observed in the slope of pressurization.

In order to simplify the analysis, the evolution of pressure and temperature is linearized in all cases. Table 3 summarizes the pressure and temperature for the different Design Basis Accident loads.

4. Cases analyzed

4.1. DBA analysis

First, boundary conditions of temperature, initial and uniform 25 ° C in the entire volume of the model were applied, as well as a boundary condition at the inner surfaces of the containment with a law of variation according to the DBA case condition

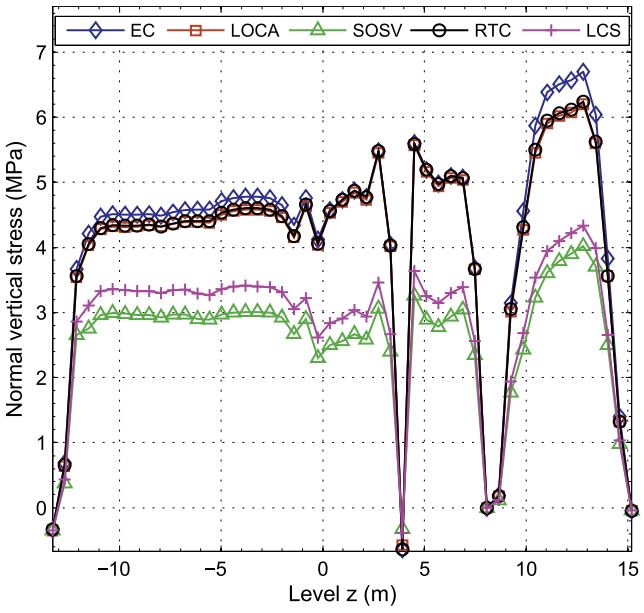

Fig. 20. Normal vertical stress. B2.

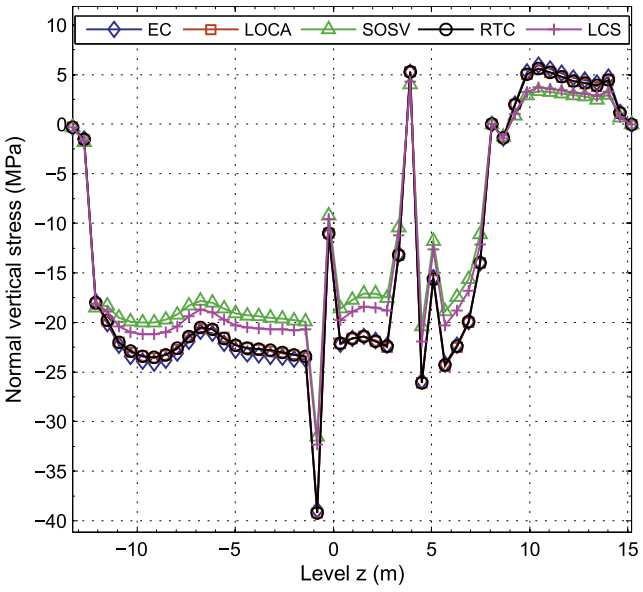

Fig. 22. Normal vertical stress. B3.

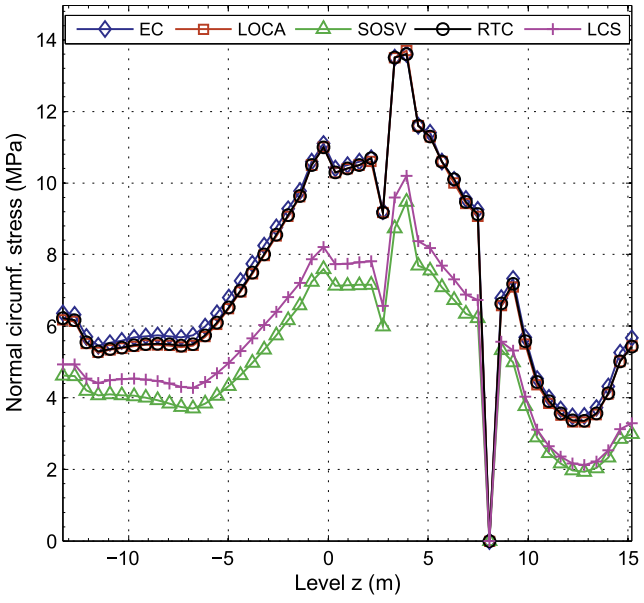

Fig. 21. Normal circumferential stress. B2.

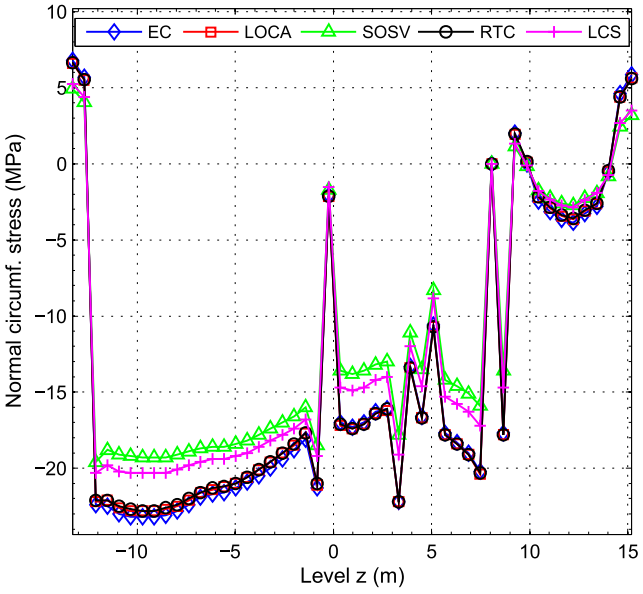

Fig. 23. Normal circumferential stress. B3.

(Table 3). Then, a transient linear thermal analysis was carried out. Thus the temporal variation (hourly) of heat conditions developed in the model, until the time recommended of a 36 h period, was evaluated. In order to analyze how temperature varies in the thickness of the wall over time, a sector of the containment free of holes and geometric discontinuities was selected. Fig. 5 shows the containment zone in which the temperature gradient in the thickness of the containment was determined. Fig. 6 presents the temperature variation in the wall thickness of the containment. Subsequently, a preliminary analysis of the temporal evolution of vertical and circumferential stresses in the same area for the DBA case was performed. Results are presented in Figs. 7 and 8.

Clearly, more sophisticated and precise thermo-mechanical analyses could be performed with the present available numerical tools (Kang et al. 2012), but the adopted methodology in this paper is considered enough precise for the objectives of the work.

As can be seen, from the middle to the outer side, the most unfavorable case occurs at 36 h. Moreover, obtaining the inner efforts such us shear forces and flexural moments, it can be demonstrated that also in the inner side of the containment can be used the 36 h case as a conservative option. Then, for design purposes, the stress state at 36 h for each load case was used.

Subsequently, a structural static analysis was performed considering the results of the 5 states of temperatures at 36 h (initial

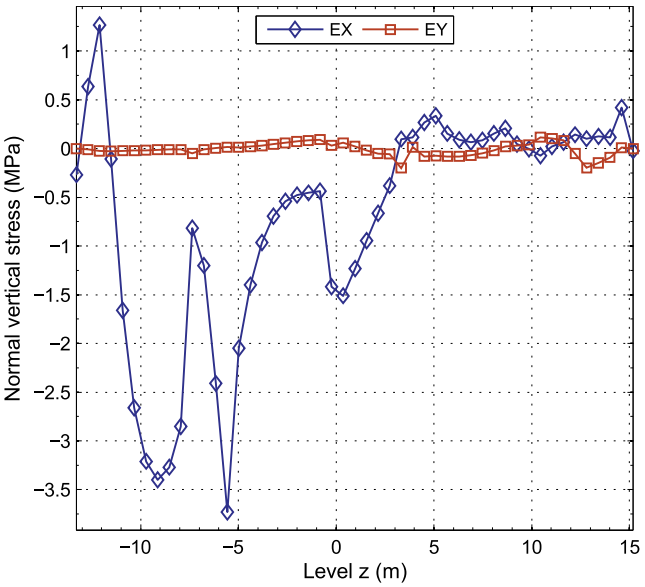

Fig. 24. Normal vertical stress. A1.

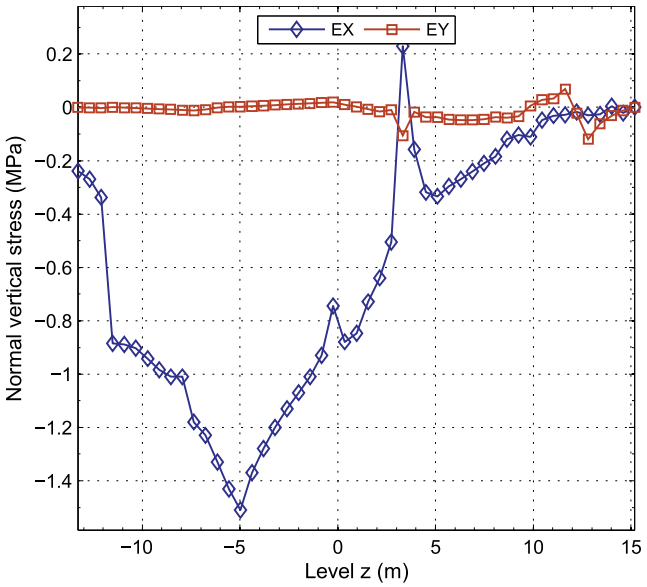

Fig. 26. Normal vertical stress. A2.

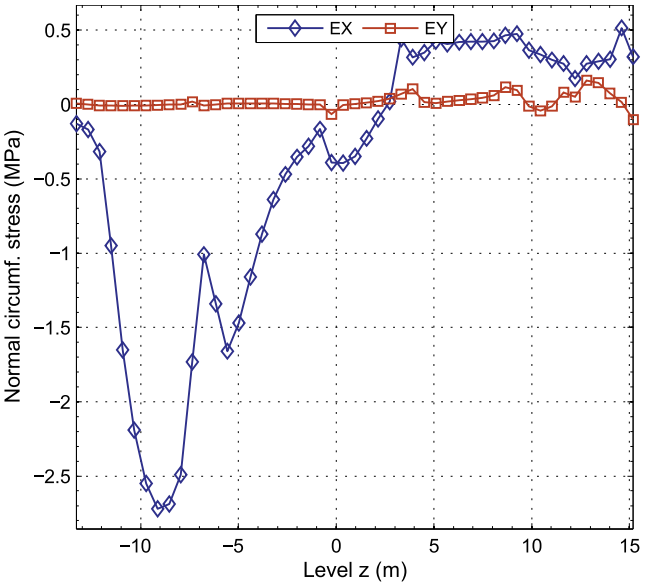

Fig. 25. Normal circumferential stress. A1.

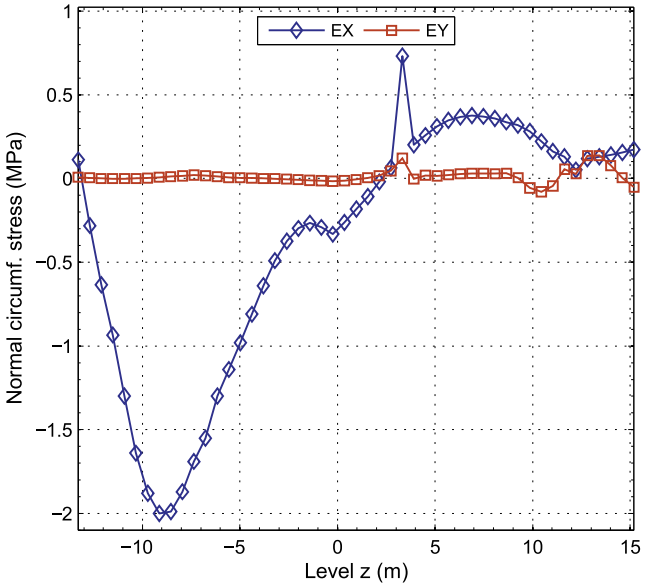

Fig. 27. Normal circumferential stress. A2.

conditions), and taking into account the pressures according to each load case (Table 3).

Taking into account that it would be very conservative to consider linear elastic state for the concrete, neglecting the stress relaxation due to the cracking, it was added this effect by mean of a simplified procedure: considering a decrease in Young's modulus. Based on results of the literature (Vecchio, 1987; Zmindák et al., 2008; James and Liu, 2009; HITACHI, 2013), $Ec = 0.65E$ was used, where Ec is the modulus of elasticity of cracked concrete.

It should be also noted that, equipment, mechanical, dead and live loads, were included in all the cases, according to the data provided by CNEA.

4.2. Modal analysis

With the objectives of determining the value of the spectral acceleration corresponding to natural frequencies of vibration in the X and Y directions and calibrating the stiffness of the foundation of the reduced model, a modal analysis was performed. First 50 modes were found, some of which correspond to local vibration modes of roof or slabs with very low participation in the structural response. Table 4 presents the natural frequencies of the fundamental modes obtained and their comparison with Soil-Structure Interaction analysis results of the complete model (Ambrosini et al., 2014).

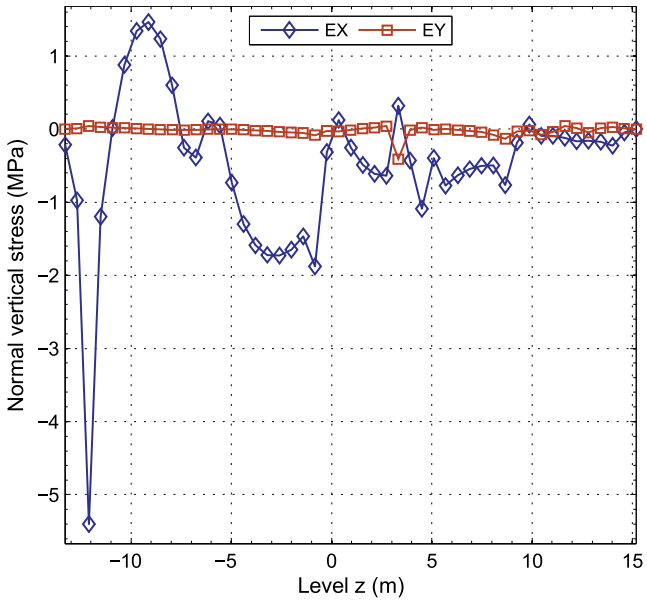

Fig. 28. Normal vertical stress. A3.

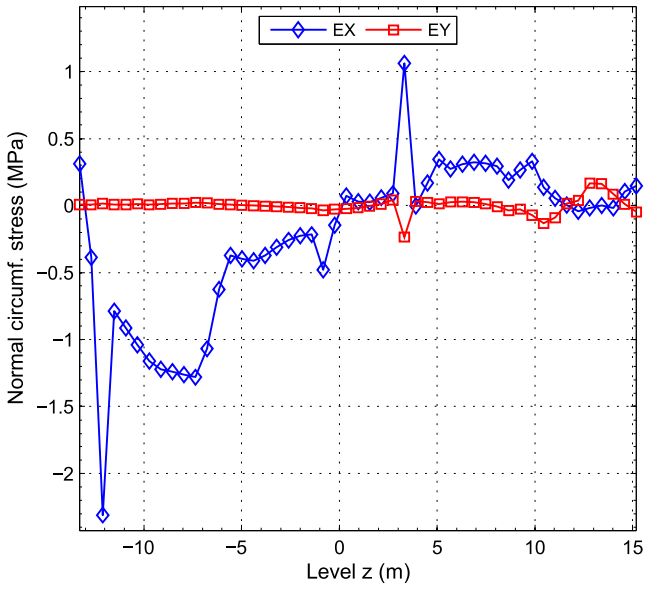

Fig. 29. Normal circumferential stress. A3.

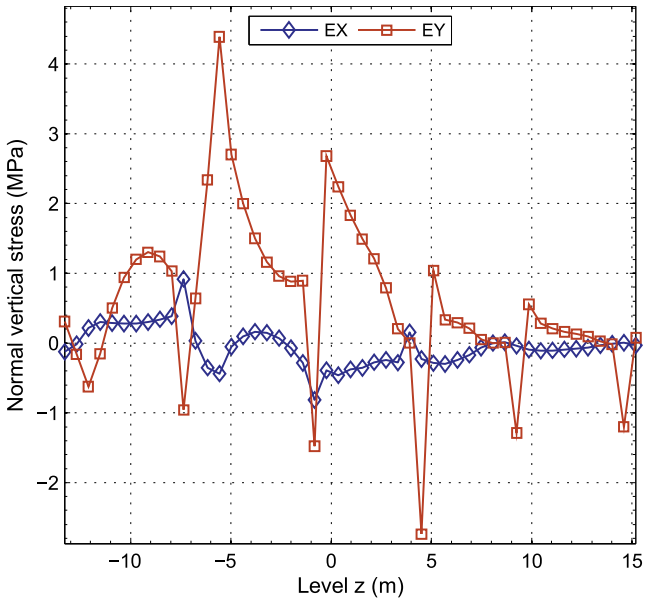

Fig. 30. Normal vertical stress. B1.

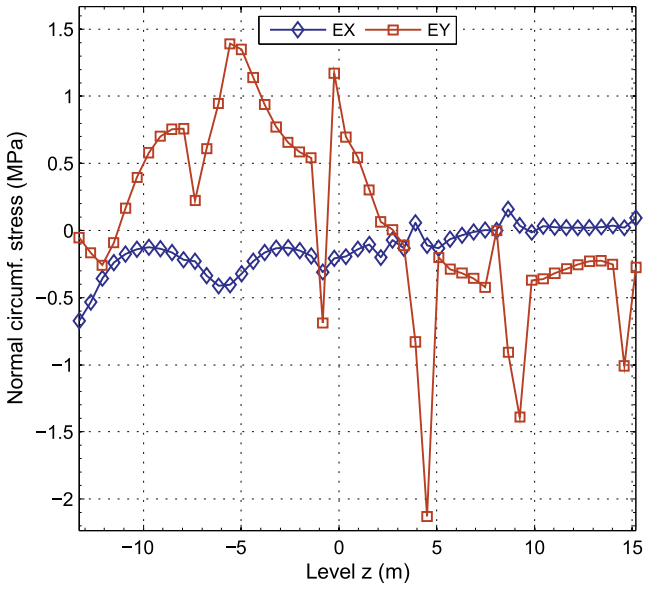

Fig. 31. Normal circumferential stress. B1.

Taking into accounts that are compared two different very complex models with millions of elements, reasonable differences in the frequencies of the fundamental modes are observed. Therefore it could be considered that the reduced model used in this analysis and presented in Fig. 1 is a good approximation of the entire building.

4.3. Seismic analysis

For the evaluation of the stress states resulting from the different seismic actions (Actions Severe Environmental and Extreme Environmental according to ASME, 2007), an equivalent static analysis was performed considering the value of the spectral acceleration obtained from the design spectrum defined in Ambrosini et al. (2014) and the values of the fundamental frequency of the translational modes in X and Y. The choice of the analysis method is based on the following reasons:

– The ratio of effective mass involved in the fundamental mode in each direction is high and therefore the error by neglecting the participation of higher modes is minimum. In addition, stresses

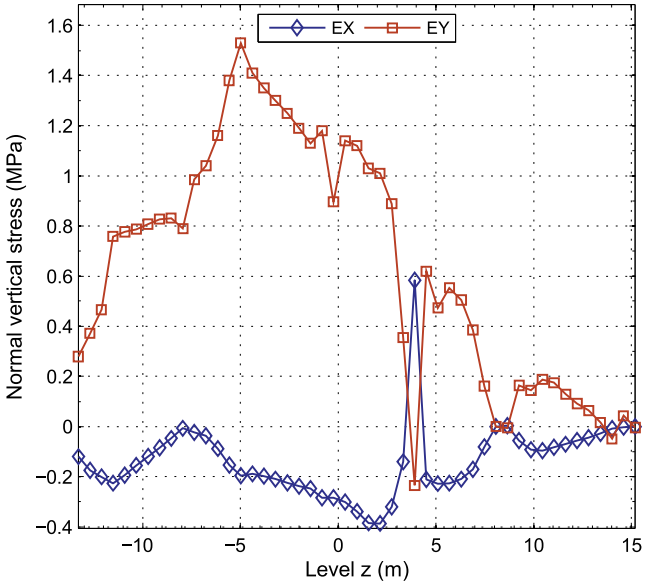

Fig. 32. Normal vertical stress. B2.

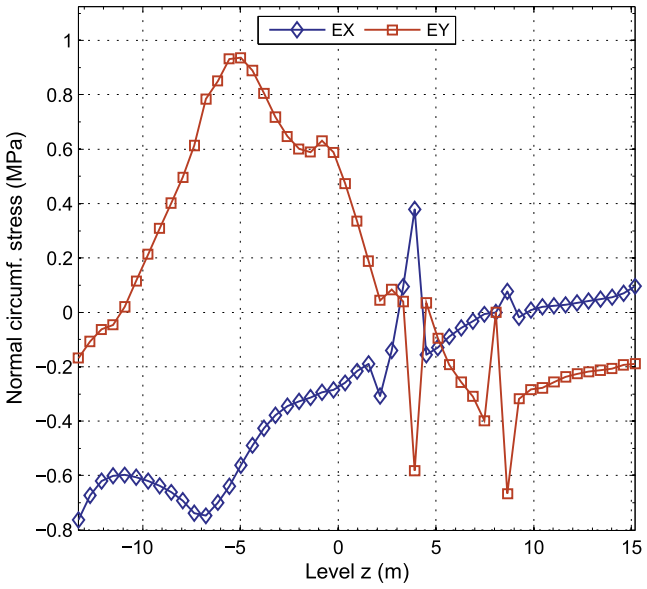

Fig. 33. Normal circumferential stress. B2.

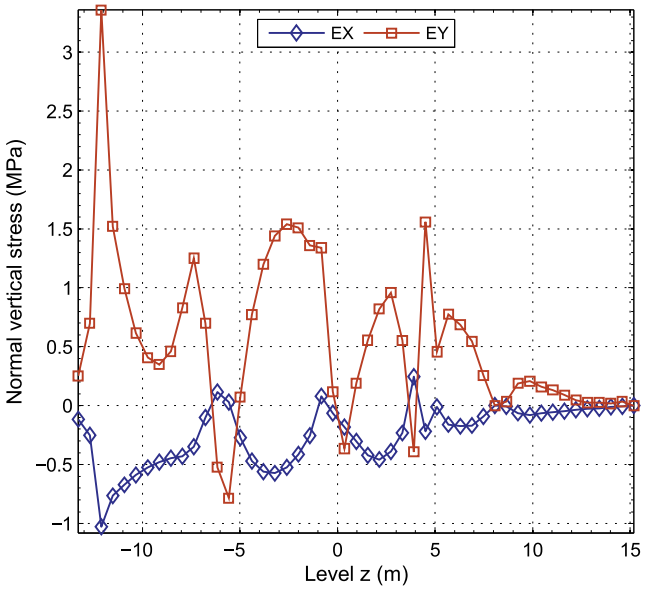

Fig. 34. Normal vertical stress. B3.

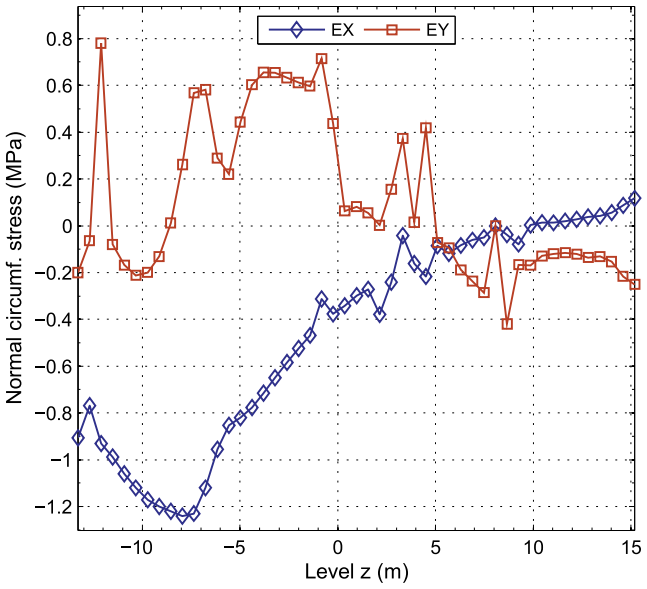

Fig. 35. Normal circumferential stress. B3.

resulting from the seismic action are low compared to thermal stresses during accident (envelope condition) as can be seen in the section 5.

– Through this method, it is possible to combine thermal, mechanical and seismic actions in different directions to obtain maps of combined stresses and deformations. Thus, it is possible to obtain a comprehensive assessment of the structural response to different load states and combinations.

The results of this equivalent static analysis were also compared with a modal spectral analysis with 50 vibration modes and the approach was considered acceptable.

4.4. Load combinations

The load combinations were performed following the recommendations of ASME (2007), using the Table CC-3230-1.

5. Numerical results

This section presents the main results obtained in the structural analysis. In order to perform an exhaustive comparison between structural responses in each state, fixed axes which intersect different areas of the cylindrical core were defined, as shown in Figs. 9 and 10.

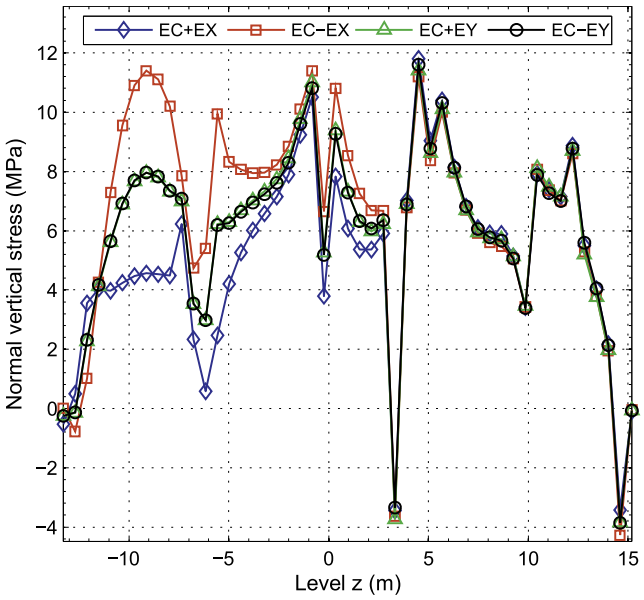

Fig. 36. Normal vertical stress. A1.

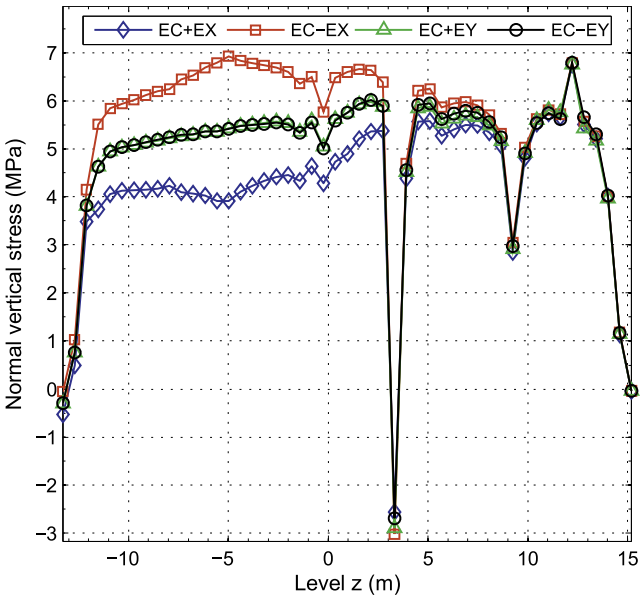

Fig. 38. Normal vertical stress. A2.

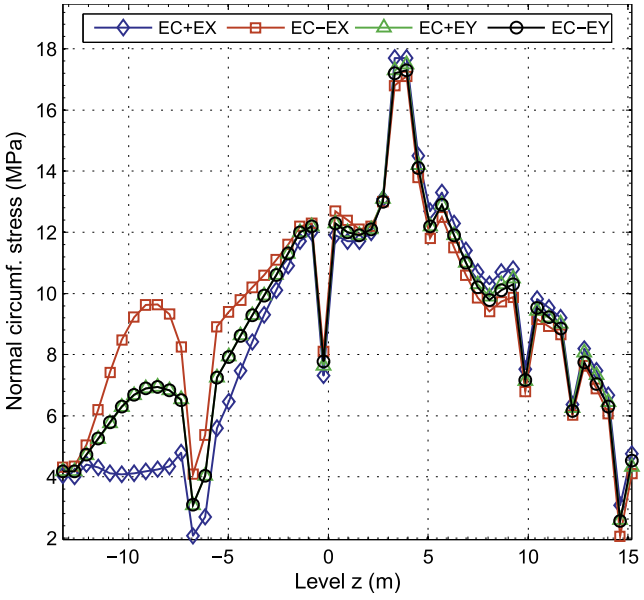

Fig. 37. Normal circumferential stress. A1.

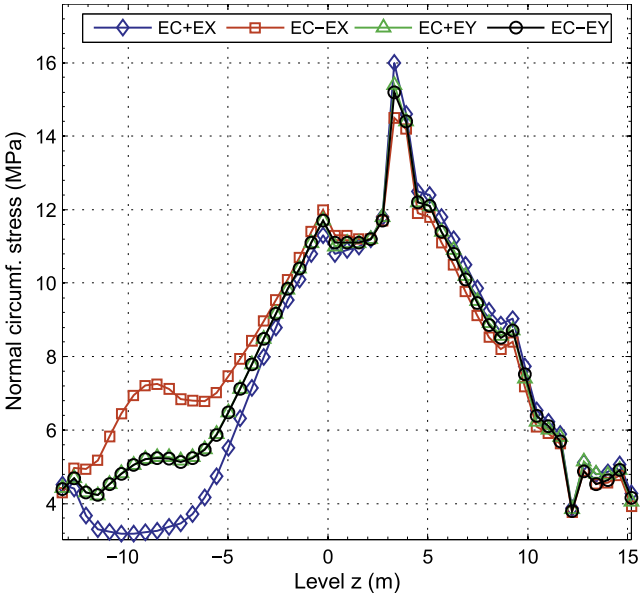

Fig. 39. Normal circumferential stress. A2.

5.1. Results of the thermo-mechanical analysis

Fig. 11 shows vertical and circumferential stresses of the internal and external faces of the containment wall.

The vertical and circumferential stresses obtained for the states listed in Table 3 for the axes A and B are shown in Figs. 12–23

Based on Figs. 12–23, the following should be noted:

a) In general, as expected, the envelope is the most unfavorable condition.
b) The stress peaks observed in some cases, correspond to stress concentrations in holes, edges, corners, stiffness discontinuity, etc. These values are unrealistic because linear elastic material is considered. In a real case, stresses will be redistributed due to local cracking of the concrete.

5.2. Results of seismic analysis

In order to present the results of seismic analysis, the same axes defined in Figs. 9 and 10 are used. The results obtained for seismic actions in X and Y directions are presented in Figs. 24–35.

As can be seen in Figs. 24–35, vertical and circumferential stresses due to seismic load, defined in ASME (2007) as safe shutdown earthquake (SSE), with a PGA of 0.25 g are one or two orders of magnitude lower than the stresses developed by the envelope condition of DBA. For this reason, it is estimated that it is not necessary to perform the analysis with the seismic action defined in ASME (2007) as operating basis earthquake (OBE), with PGA = 0.05 g, because the values of stresses generated by this action will be negligible respect to the DBA condition.

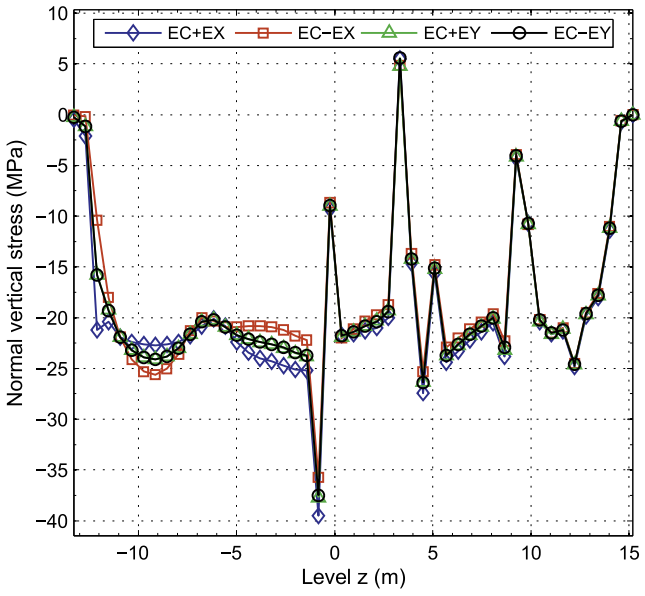

Fig. 40. Normal vertical stress. A3.

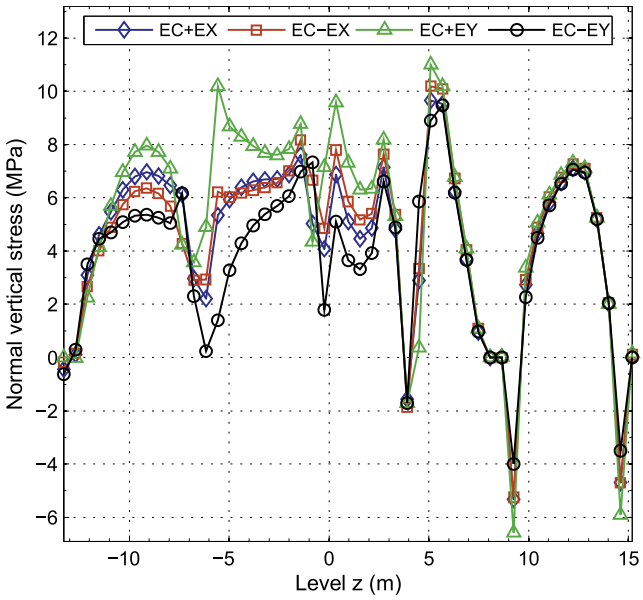

Fig. 42. Normal vertical stress. B1.

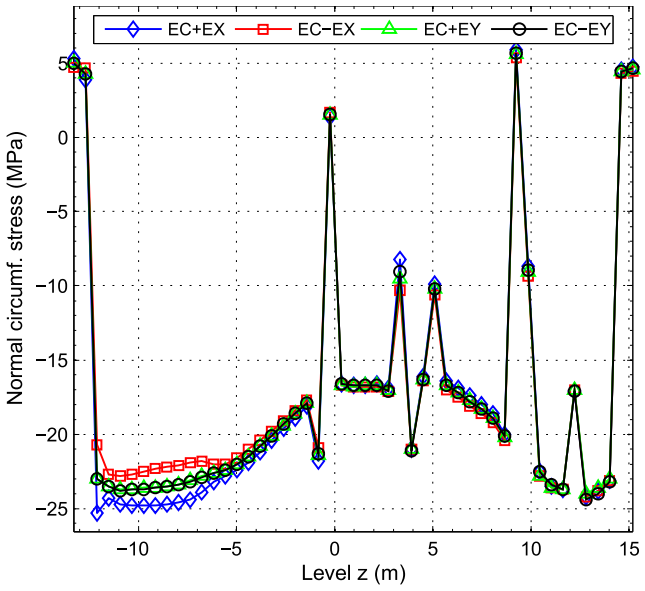

Fig. 41. Normal circumferential stress. A3.

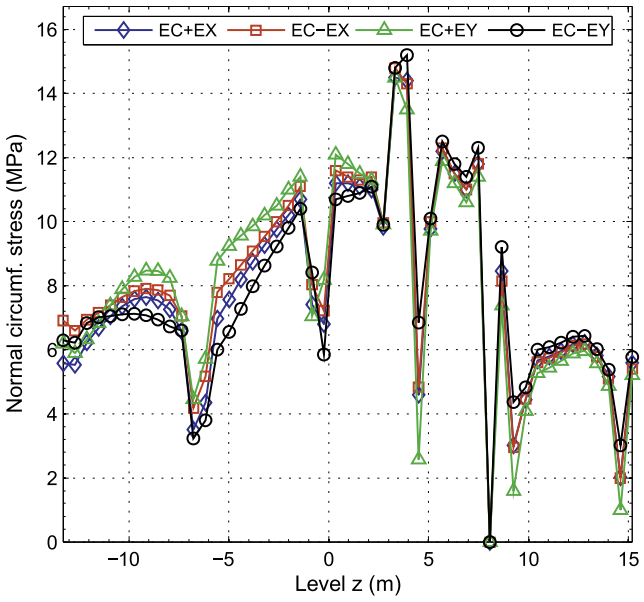

Fig. 43. Normal circumferential stress. B1.

5.3. Results of load combinations

Given that the DBA are clearly those that produce greater stresses and, among these, the envelope is the most unfavorable condition, verifications are made in this point for the Abnormal/Extreme Environmental combination (ASME, 2007). Figs. 36–47 present the values of vertical and circumferential stresses in the selected axes for the Abnormal/Extreme Environmental condition (Envelope Condition ± Safe Shutdown Earthquake, PGA = 0.25 g in both horizontal directions, X and Y).

Analyzing Figs. 36–47 and comparing these results with those obtained from the envelope condition (Figs. 12–23) it is clear that the envelope condition produces practically the same stresses as those obtained by the load combinations.

6. Conclusions

In this paper, the structural response of the concrete reactor containment of CAREM-25 subjected to thermal, mechanical and seismic loading was presented. For this purpose, a full 3D numerical model was developed and transient thermal and static structural analyses were performed.

Vertical, circumferential and radial stresses, in different axes of the containment cylinder, were obtained. They allowed establishing complete stress state of the containment structure. Load combinations established by ASME (2007) were performed.

At first, it was established that a size of elements of 20 cm is enough to obtain accurate results. On the other hand, it can be seen that temperatures at 36 h produces the most unfavorable stress

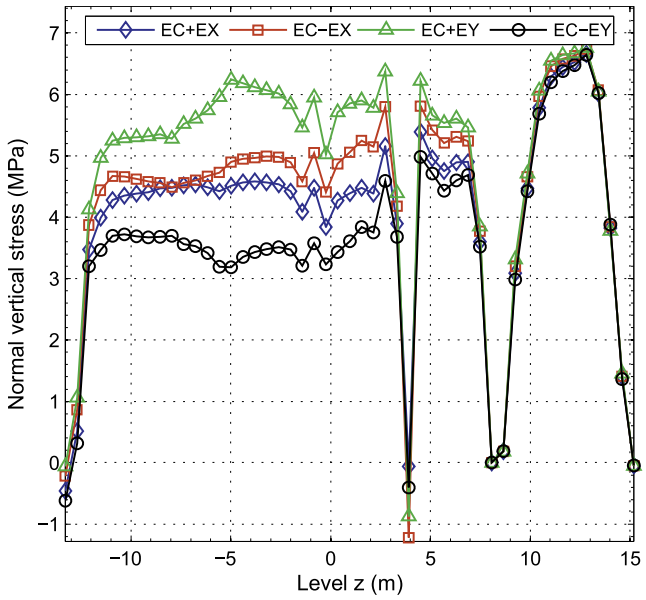

Fig. 44. Normal vertical stress. B2.

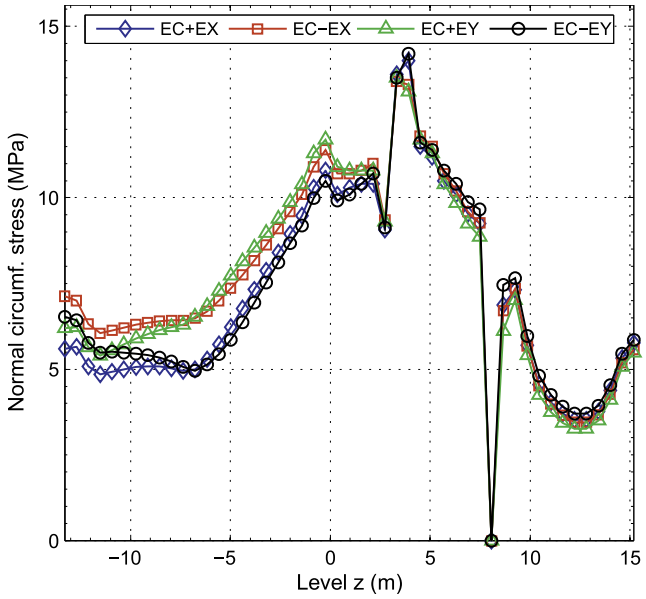

Fig. 45. Normal circumferential stress. B2.

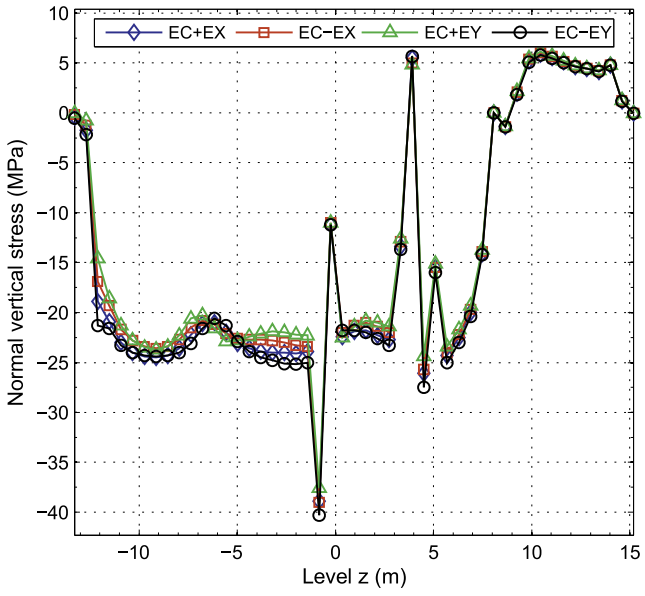

Fig. 46. Normal vertical stress. B3.

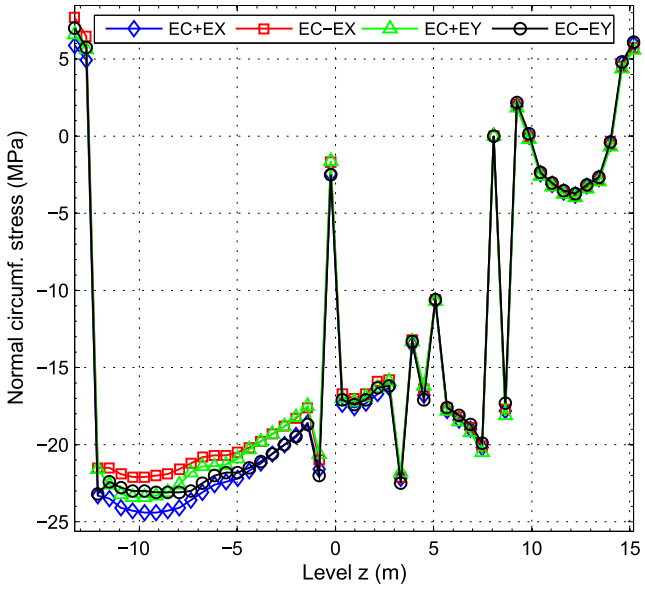

Fig. 47. Normal circumferential stress. B3.

state. Moreover, it was verified that the envelope condition of DBA dominates the behavior and therefore the containment structural design.

Regarding to compressive stresses, it can be seen that using a concrete of 40 MPa compressive strength or more, appropriate levels of structural safety will be achieved. For tensile stresses, the distribution of the same shows how the reinforcement should be detailed at different levels. Finally, according to expected stress concentrations in holes, edges, stiffness changes, etc. were observed; which are locally redistributed due to cracking of concrete and, in some cases, will require a special detailing of the reinforcement around singularities.

Results showed that stresses arising from seismic actions are negligible compared to those generated by DBA.

Acknowledgements

The financial support of CONICET and National University of Cuyo is gratefully acknowledged. Special acknowledgements are extended to Eng. Ignacio de Arenaza and Eng. Martín Arribas from CNEA, Argentina.

References

ACI (American Concrete Institute), 2001. Code Requirements for Nuclear Safety Related Concrete Structures. ACI 349–01. Reported by ACI Committee 349, 2001.

ACI (American Concrete Institute), 2007. Reinforced Concrete Design for Thermal Effects on Nuclear Power Plant Structures. ACI 349.1R-07. Reported by ACI Committee 349, 2007.

Ambrosini, D., Curadelli O, de Borbón, F., Domizio, M., 2014 Seismic analysis of CAREM25 nuclear power plant considering soil structure interaction, XXXVI Jornadas Sudamericanas de Ingeniería Estructural, Montevideo, Uruguay, Nov 2014, pp. 1–15. (in Spanish).

ANSYS, 2010. User Manual, Version 13.0, ANSYS Inc, USA. 2010.

ASME (American Society of Mechanical Engineers), 2007. Boiler & Pressure Vessel Code, Section III, Division 2: Code for Concrete Containments, ACI-ASME Joint Technical Committe, Ed. 2007.

Boado Magan, H., Delmastro, D.F., Markiewicz, M., Lopasso, E., Diez, F., Giménez, M., Rauschert, A., Halpert, S., Chocrón, M., Dezzutti, J.C., Pirani, H., Balbi, C., Fittipaldi, A., Schlamp, M., Murmis, G.M., Lis, H., 2011. CAREM project status. Sci. Tech. Nucl. Installations 2011, 1–6.

CNEA (National Atomic Energy Commission), 2011. Load states related to Design Base Events to be considered in the structural design of the containment from the point of view of Nuclear Safety. Report MEM-CAREM25S-14 (in Spanish), 2011.

CNEA (National Atomic Energy Commission), 2012. Revision of load states related to Design Base Events to be considered in the structural design of the containment from the point of view of Nuclear Safety (First part), Report MEM-CAREM25S-19 (in Spanish), 2012.

CNEA (National Atomic Energy Commission), 2012. Revision of load states related to Design Base Events to be considered in the structural design of the containment from the point of view of Nuclear Safety (Second part), Report MEM-CAREM25S-20 (in Spanish), 2012.

CNEA (National Atomic Energy Commission), 2013. Update of load states to be considered in the design of the containment, Report IN-CAREM25C-10 (in Spanish), 2013.

Delmastro, D.F., 2000. Thermal-hydraulic aspects of CAREM reactor. In: Proceedings of the IAEA TCM on Natural Circulation Data and Methods for Innovative Nuclear Power Plant Design, Vienna, Austria.

HITACHI, 2013. 26A6642BY Rev. 10. ESBWR Design Control Document. Tier 2. Chapter #19. Probabilistic risk assessment and severe accidents. Sections 19.1 – 19.5 and Appendices; December 2013.

James, R., Liu, A., 2009. Nonlinear analyses for thermal cracking in the design of concrete structures. In: Proceedings of the 17th International Conference on Nuclear Engineering ICONE17- 75474. Brussels, Belgium, July 12-16, 2009.

Kang, J., Tak, N., Kim, M., 2012. Thermo-mechanical analysis of the prismatic fuel assembly of VHTR in normal operational condition. Ann. Nucl. Energy 92 (113–126), 2016.

Kwak, H., Kwon, Y., 2016. Nonlinear analysis of containment structure based on modified tendon model. Ann. Nucl. Energy 44 (76–86), 2012.

Li, Q., Yuan, L., Ansari, F., 2002. Model for measurement of thermal expansion coefficient of concrete by fiber optic sensor. Int. J. Solids Struct. 39 (2927–2937), 2002.

Marcel, C.P., Furci, H.F., Delmastro, D.F., Masson, V.P., 2013. Phenomenology involved in self-pressurized, natural circulation, low thermo-dynamic quality, nuclear reactors: The thermal–hydraulics of the CAREM-25 reactor. Nucl. Eng. Des. 2013 (254), 218–227.

Neville, A.M., 1995. Properties of Concrete. John Wiley & Sons, New York, p. 1995.

Uygunoglu, T., Topçu, B., 2009. Thermal expansion of self-consolidating normal and lightweight aggregate concrete at elevated temperature. Constr. Build. Mater. 23 (3063–3069), 2009.

Vecchio, F., 1987. Nonlinear analyses of reinforced concrete frames subjected to thermal and mechanical loads. ACI Struct. J., 492–501 Technical paper. Title no. 84-S51.

Willam, K., Xi, Y., Lee, K., Kim, B., 2009. Thermal response of reinforced concrete structures in nuclear power plants. SESM No. 02–2009. Department of Civil, Environmental, and Architectural Engineering College of Engineering and Applied Science. University of Colorado at Boulder, 2009.

Wolf, J.P., Somaini, D., 1986. Approximate dynamic model of embedded foundation in time domain. Earthquake Eng. Struct. Dyn. 1986 (14), 683–703.

Yu, Y., Lv, X., Niu, F., 2015. Large LOCA accident analysis for AP1000 under earthquake. Ann. Nucl. Energy 77 (142–147), 2015.

Zmindák, M., Novák, P., Nozdrovický, J., 2008. Thermo-mechanical transient analysis of concrete structure around the nuclear reactor. Appl. Comput. Mech. 2 (409–418), 2008.